New Journal of Physics
The open-access journal for physics

Attosecond control of electron–ion recollision in high harmonic generation

G Gademann[1,6], F Kelkensberg[1], W K Siu[1], P Johnsson[2], M B Gaarde[3,4], K J Schafer[3,4] and M J J Vrakking[1,5]

[1] FOM—Institute for Atomic and Molecular Physics (AMOLF), Science Park 104, 1098 XG Amsterdam, The Netherlands
[2] Department of Physics, Lund University, PO Box 118, SE-22100 Lund, Sweden
[3] Department of Physics and Astronomy, Louisiana State University, Baton Rouge, LA 70803-4001, USA
[4] PULSE Institute, SLAC National Accelerator Laboratory, Menlo Park, CA 94025, USA
[5] Max-Born-Institut für Nichtlineare Optik und Kurzzeitspektroskopie, Max-Born-Straße 2A, 12489 Berlin, Germany
E-mail: g.gademann@amolf.nl

New Journal of Physics **13** (2011) 033002 (8pp)
Received 10 November 2010
Published 1 March 2011
Online at http://www.njp.org/
doi:10.1088/1367-2630/13/3/033002

Abstract. We show that high harmonic generation driven by an intense near-infrared (IR) laser can be temporally controlled when an attosecond pulse train (APT) is used to ionize the generation medium, thereby replacing tunnel ionization as the first step in the well-known three-step model. New harmonics are formed when the ionization occurs at a well-defined time within the optical cycle of the IR field. The use of APT-created electron wave packets affords new avenues for the study and application of harmonic generation. In the present experiment, this makes it possible to study harmonic generation at IR intensities where tunnel ionization does not give a measurable signal.

High harmonic generation (HHG) is well-known for producing attosecond pulse trains (APTs) and individual attosecond pulses [1, 2]. In the language of the semi-classical three-step model of harmonic generation, an electron is released into the continuum via tunnel ionization, gains kinetic energy via acceleration in the laser field and, upon rescattering with the parent ion,

[6] Author to whom any correspondence should be addressed.

can recombine and give rise to emission of high-frequency radiation [3, 4]. The recolliding electron wave packet (EWP) can be viewed as a probe for the generating system, offering the possibility of four-dimensional (4D) imaging with angstrom spatial and attosecond temporal resolutions [5]–[8]. Until now, the only temporal control over the HHG process has come via the shaping of the strong infrared (IR) laser field that drives all three steps in the process [9], with the constraint that the peak intensity must be high enough to drive the initial ionization step.

By generating harmonics with an APT in combination with an IR pulse, the IR-driven tunnel ionization step in the three-step model can be replaced by APT-driven one-photon ionization. The technique of using an APT to control the initial EWP in harmonic generation was first proposed in theoretical works in 2004 [10]. The short duration and high photon energy of the individual pulses in the APT allow the ionization to be fixed to a certain time during the IR cycle, which can be controlled via the relative delay between the two pulses. The APT ionization allows direct control over the initial EWP, and the IR field will subsequently control the acceleration and potential recollision of the EWP. A similar APT–IR control scheme was used experimentally in [11, 12] to create and control below-threshold EWPs in helium in order to study time-dependent coherent electron rescattering on the parent ion. Biegert *et al* [13] demonstrated a strong enhancement of harmonics generated in helium in a two-colour IR–APT experiment in which the relative delay between the IR and APT pulses was not controlled.

In this paper, we demonstrate for the first time that it is possible to temporally control HHG by forming the initial EWP with an APT. To do this, we first synthesize an APT via harmonic generation in xenon using a strong IR laser pulse. The APT is inherently synchronized to this IR field [14]. We then use the APT and a copy of the IR pulse, which is independently delayed relative to the APT, to generate harmonics in helium in a separate gas jet. We show that the helium harmonics are enhanced periodically as a function of the APT–IR delay, with a maximum in the efficiency occurring once every half-optical cycle of the IR field. The enhancement occurs when the extreme ultraviolet (XUV) ionization launches the EWP on a trajectory which can return to the core [10]. Moreover, under our experimental conditions the kinetic energy of the APT-initiated returning EWPs is in a range that is not accessible in EWPs launched by IR tunnel ionization. We show that the experimental results are in good agreement with calculations including both the single-atom and macroscopic responses. Our results demonstrate that it is possible to decouple the ionization step from the acceleration and rescattering steps in the three-step harmonic generation process, offering a new degree of control over initial and rescattering EWPs.

The experiments were conducted with a 780 nm IR laser system that delivered 30 fs laser pulses with a pulse energy of 2 mJ at a repetition rate of 3 kHz. 50% of the beam was used to generate the initial APT in a 3 mm long gas cell filled with xenon. The low-order harmonics and the remaining IR after the first gas cell were filtered out with a 200 nm Al filter. The resulting APT comprised of harmonics 11–21 was propagated to a second 3 mm long gas cell filled with helium (15–25 mbar), where it was collinearly recombined with the remaining IR beam from the other interferometer arm. The focusing conditions of the two beams were adjusted such that the beams focused slightly before the second gas cell to favour phase matching of the short electron trajectories [15]. The relative APT–IR delay could be adjusted over several hundreds of femtoseconds with a resolution of less than 100 as (see figures 1 and 2) by actively stabilizing the interferometer arms. In the absence of temporal overlap between the IR and APT pulses, the helium gas is observed to absorb only harmonics 17–21 of the APT, which are above the

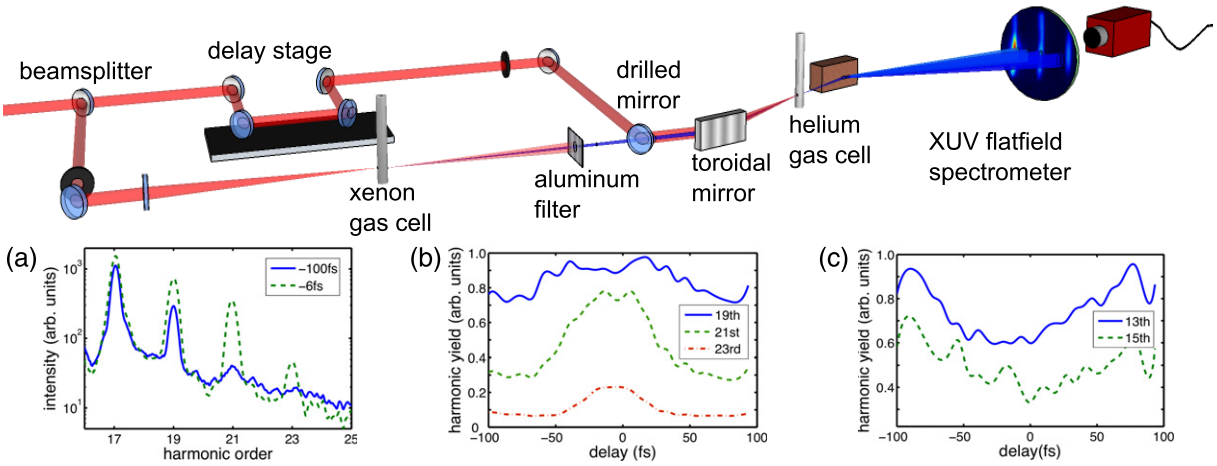

Figure 1. (Top) Schematic drawing of the experimental setup. (Bottom) Raw data of measurements scanning over a large delay range. (a) Two individual spectra taken far away from and close to temporal APT–IR overlap. The background at large delays and high energies is due to scattered XUV light from blocked out lower harmonic orders. At temporal overlap these orders will be depleted by enhanced absorption, as seen in figure 1(c), thus reducing the background for measurements at temporal overlap. (b) Coarse delay scan of the yield of harmonics 19, 21 and 23 showing a strong enhancement. (c) Harmonics 13 and 15 as a function of the APT–IR delay, revealing absorption when the two pulses overlap.

He ionization threshold. When the XUV and IR pulses are overlapped, we also observe strong absorption of harmonics 13 and 15, indicating that the APT-driven ionization of the laser dressed atom is due to the simultaneous absorption of several harmonics and therefore of short duration (see figure 1(c)).

The spectra in figure 1(a) show the harmonic yield for harmonics 17–23 for two different APT–IR delays. Negative delays indicate that the IR pulse precedes the APT. For large time delays, when there is no temporal overlap, only harmonic orders of the original APT are detected behind the second gas cell. The IR pulses by themselves are too weak to produce harmonics. At temporal overlap of the APT and the IR pulse, however, new harmonics 23–27 can be observed (see figures 1(a) and 3(a)). In addition, the yield of existing harmonics 17–21 is significantly enhanced.

Figure 2 shows a sub-cycle delay scan of the yield of harmonics 19–23, performed around zero temporal APT–IR overlap. All three harmonics clearly exhibit periodic enhancement once per half-cycle of the IR field. At these delays, the APT not only increases the probability for one-photon ionization as compared to IR tunnel ionization, but also launches the EWP onto a returning trajectory, thereby enhancing the yield of these harmonic orders. In the semi-classical model the release times that lead to returning electrons are controlled by the IR field and are directly related to the electron's energy upon return [10, 16]. By fitting sine functions to the experimental data and extracting the respective phase, we observe a clear delay between the optimal release times of harmonics 19 and 21 (120 as delayed from H19) and 23 (270 as delayed from H19). Also shown in the figure is a calculated delay scan, which will be discussed in further detail below.

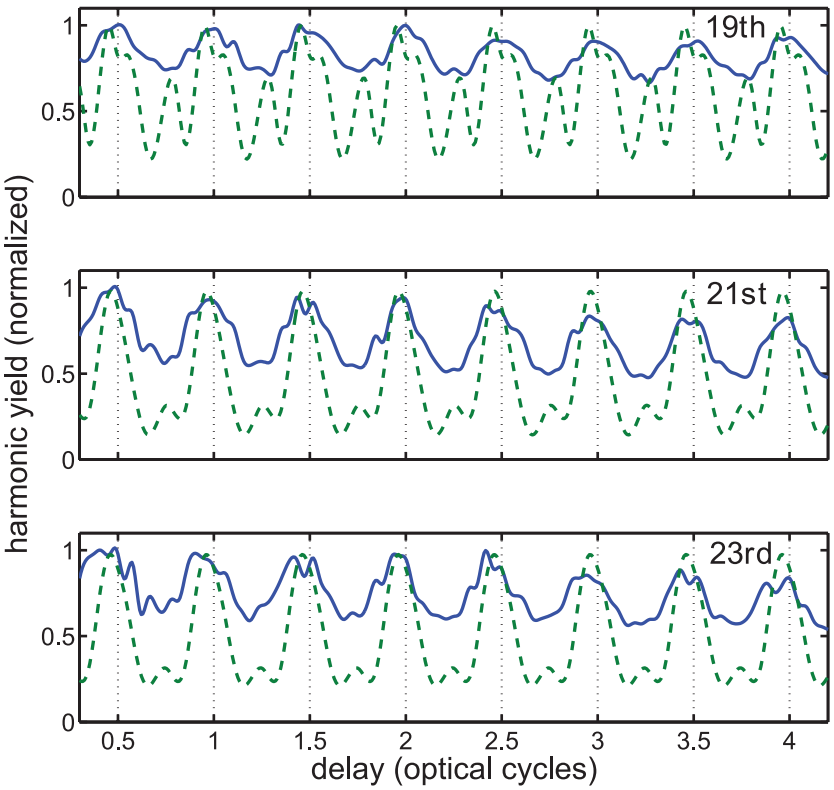

Figure 2. High-resolution delay scan of the yield of harmonics 19, 21 and 23, with the delay given in units of the IR cycle. The experimental (blue solid line) and the theoretical results (green dashed line) agree well.

Figure 3 shows a spectrum and a delay scan measured in an experimental configuration where the IR focus was moved 6 mm toward the gas jet, which in general leads to improved phase matching of the long trajectory contribution to the harmonic spectrum [15]. The spectrum in figure 3(a) has a higher cutoff energy than the measurements of figure 1 because of the increase in IR intensity in the gas jet. In addition, a new spectral feature has appeared in harmonics 23–27 on the low-energy side of each harmonic. In figure 3(b), we separate the time dependence of the two features by showing a delay scan of each of the two spectral features for harmonic 25 (highlighted in different colours in figure 3(a)), obtained by spectral integration over each region separately for each delay-dependent spectrum. We attribute the blue contribution as coming from short trajectory returns, and the red contribution, which is observed predominantly off-axis and is only visible in this phase-matching configuration, as coming from long trajectory returns. Figure 3(b) shows that the long trajectory contribution is shifted by 350 as with respect to the short trajectory contribution, consistent with the expectation from the semi-classical model in which long trajectories are released earlier than short trajectories [10, 17]. This behaviour is also reproduced in calculations described in more detail below (theoretical results not plotted in figure 3(b)).

To gain a more complete understanding of our experimental results, we have performed a series of calculations including the combined microscopic and macroscopic responses of the helium gas to the combined IR–APT fields. We solve the coupled Maxwell wave equation and

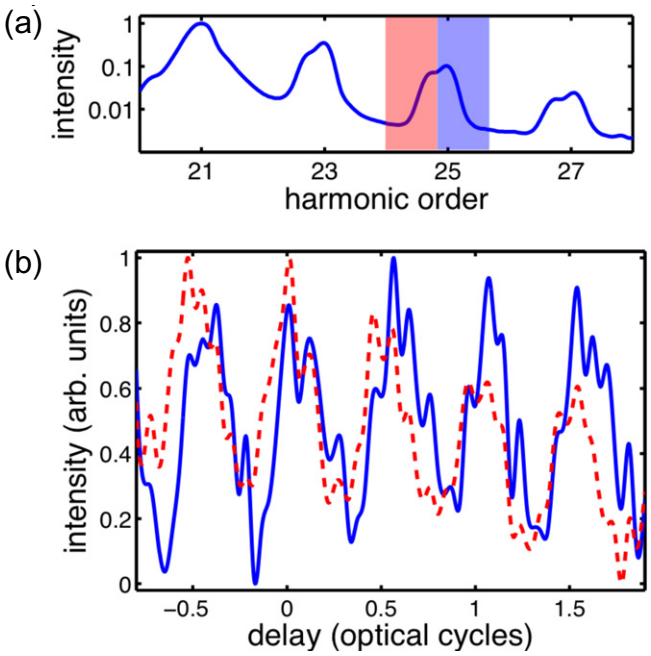

Figure 3. (a) Typical harmonic spectrum at a harmonic yield maximum for phase matching with long trajectory contributions. Sidebands (red area) below the short trajectory (blue area) signal appear and are enhanced for certain delays. (b) The delay dependence for short (blue solid line) and long (red dashed line) trajectories is shown using the example of harmonic 25. The two contributions are out of phase by 350 as. The two signals have been normalized to their respective maximum and minimum values to emphasize their relative temporal shift.

the time-dependent Schrödinger equation (TDSE) for all frequencies ω of the combined electric field $E_{\rm tot}(\omega)$, composed of the IR probe, the seeding APT and the generated harmonics:

$$\nabla_{\perp}^{2} E_{\rm tot}(\omega) + \frac{2{\rm i}\omega}{c} \frac{\partial E_{\rm tot}(\omega)}{\partial z} = -\omega^{2} \mu_{0} (P(\omega) + P_{\rm ion}(\omega)).$$

$E_{\rm tot}$ and the P terms are also functions of the cylindrical coordinates r and z. We solve this equation by space-marching through the helium gas, at each plane z in the propagation direction calculating the response $P(\omega)$ as the Fourier transform of the time-dependent dipole moment (times the atomic density) driven by the evolving electric field $E_{\rm tot}(t)$. The dipole moment is calculated via numerical integration of the TDSE within the single active electron (SAE) approximation. The source term is then used to propagate to the next plane in z, thereby coupling the harmonics generated in one step back into the full electric field so that they will contribute to the driving electric field in the next step. In this way, we obtain a very complete description of both the single-atom harmonic generation and the macroscopic phase matching, absorption and dispersion imprinted on the harmonics in the gas medium. The term $P_{\rm ion}(\omega)$ is due to the free-electron plasma current and is also calculated within the TDSE-SAE, see [18]. This term is very small in our experimental configuration.

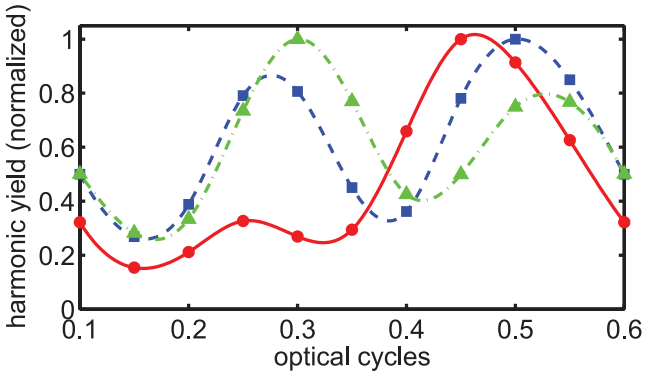

Figure 4. Calculated delay dependence of H21 yield for IR intensities of 5×10^{13} W cm^{-2} (red solid line), 6.5×10^{13} W cm^{-2} (blue dashed line) and 7.5×10^{13} W cm^{-2} (green dash-dotted line). As the intensity increases the yield is enhanced twice per half-cycle, as opposed to once per half-cycle at low intensities.

The green curves in figure 2 show the calculated delay dependence of harmonics 19–23 in conditions similar to the experiment. The peak intensity of the IR (APT) pulse is 5×10^{13} W cm^{-2} (5×10^{9} W cm^{-2}), with a duration of 26 fs (13 fs). The beam focal diameters are 100 μm (40 μm). The APT is synthesized from harmonics 11–19, with relative strengths obtained from the experiment and with relative phases consistent with the semi-classical model [16]. The individual bursts in the APT are thus strongly chirped with a duration of approximately 430 as. The 3 mm long He jet is placed 4 mm downstream from both laser focii. In figure 2, delays of 0.0, 0.5, etc mean that the attosecond bursts overlap the peaks of the IR electric field in the common focus of the two beams. Because of the different Guoy phase shifts of the two beams, the overlap in the generation medium of the APT and the peak IR field is shifted to –0.06, +0.44, +0.94, etc. In figure 2, the experimental results have been shifted in time for best overlap with the calculations. The theoretical and experimental results match well, exhibiting one enhancement peak per IR half-cycle, although the contrast is significantly higher in the theory results. The smaller secondary enhancement of H19 in the calculation is due to interference between the initial H19 radiation, included in the APT, and the newly generated H19. In the calculation the secondary peak goes away when we decrease the relative amount of H19 in the APT.

One of the most striking features of our experimental and theoretical results is that the harmonics are enhanced just once during each half-cycle of delay between the IR and APT fields. This differs from an earlier theoretical prediction of a twice-per-half-cycle enhancement of the harmonic signal in [10], corresponding to the release of the EWP initially moving uphill or downhill with respect to the IR laser force at the time of release. Our calculations show that the once-per-cycle enhancement is a consequence of the relatively low IR intensity used in our experimental conditions. Figure 4 shows that as the IR intensity is increased slightly, to 6.5 and then 7.5×10^{13} W cm^{-2}, the calculated delay dependence of harmonic 21 starts to exhibit two peaks per IR half-cycle, as predicted by the simple model in [17]. We have performed extensive calculations on the effect of experimental uncertainties on the signal-to-noise ratio in figure 2. We have in particular investigated whether imperfect spatial APT–IR overlap, or very long and/or chirped individual APT bursts, could lead to the appearance of just one enhancement

peak per half-cycle. While these effects certainly do decrease the signal-to-noise ratio, it is only at the lowest IR intensities that we observe the suppression of one of these enhancements. We attribute the observation of a once-per-half-cycle modulation to the enhanced role played by the atomic potential at low IR intensity. At low intensity the barrier formed by the combined laser and atomic potential is only weakly suppressed, which means that the electrons are released into the continuum with relatively low velocity [10]. In a separate study of classical trajectory dynamics in the combined laser and atomic potentials, we have found that uphill trajectories in particular are sensitive to the atomic potential and can rescatter many times on the core [19], suggesting that they may become trapped and not contribute to harmonic generation. Such a trapping of uphill trajectories has been observed previously when photoelectrons are launched near the ionization threshold in the presence of a dc electric field [20]. We note that without the APT it would not be possible to study harmonic generation in helium at these low intensities, since the ionization rate in helium due to the IR laser alone is prohibitively small.

The use of APT-created EWPs affords new avenues for the study and application of harmonic generation in atomic and molecular systems. For example, the study of multichannel dynamics in molecular systems could be advanced by using the large bandwidth of the APT to create an EWP, which is a coherent superposition of contributions from multiple orbitals. In addition, decoupling of the ionization and acceleration/recombination steps allows for the use of flexible polarization geometries, which, in combination with molecular alignment techniques, could significantly extend tomographic imaging of the (time-evolving) electronic orbitals [21].

Acknowledgments

This work is part of the research programme of the 'Stichting voor Fundamenteel Onderzoek der Materie (FOM)', which was supported financially by the 'Nederlandse organisatie voor Wetenschappelijk Onderzoek (NWO)'. MBG and KJS acknowledge support from the National Science Foundation through grant numbers PHY-0449235 and PHY-0701372 and from the PULSE Institute at Stanford University. High-performance computational resources were provided by the Louisiana Optical Network Initiative, www.loni.org. PJ acknowledges support from the Swedish Research Council and the Swedish Foundation for Strategic Research.

References

[1] Paul P M, Toma E S, Berger P, Mullot G, Augé F, Balcou Ph, Muller H G and Agostini P 2001 Observation of a train of attosecond pulses from high harmonic generation *Science* **292** 1689–92

[2] Kienberger R, Goulielmakis E, Uiberacker M, Baltuska A, Yakovlev V, Bammer F, Scrinzi A, Westerwalbesloh T, Kleineberg U and Heinzmann U 2004 Atomic transient recorder *Nature* **427** 817–21

[3] Corkum P B 1993 Plasma perspective on strong-field multiphoton ionization *Phys. Rev. Lett.* **71** 1994–7

[4] Schafer K J, Yang B, DiMauro L F and Kulander K C 1993 Above threshold ionization beyond the high harmonic cutoff *Phys. Rev. Lett.* **70** 1599–602

[5] Niikura H, Légaré F, Hasbani R, Bandraik A D, Ivanov M Yu, Villeneuve D M and Corkum P B 2002 Sub-laser-cycle electron pulses for probing molecular dynamics *Nature* **417** 917–22

[6] Kanai T, Minemoto S and Sakai H 2005 Quantum interference during high-order harmonic generation from aligned molecules *Nature* **435** 470–4

[7] Baker S, Robinson J S, Harworth C A, Teng H, Smith R A, Chirila C C, Lein M, Tisch J W G and Marangos J P 2006 Probing proton dynamics in molecules on a attosecond time scale *Science* **312** 424–7

[8] Smirnova O, Mairesse Y, Patchkovskii S, Dudovich N, Villeneuve D, Corkum P and Ivanov M Yu 2009 High harmonic interferometry of multi electron-dynamics in molecules *Nature* **460** 972–7
[9] Mauritsson J, Johnsson P, Gustafsson E, L'Huillier A, Schafer K J and Gaarde M B 2006 Attosecond pulse trains generated using two color laser fields *Phys. Rev. Lett.* **97** 13001
[10] Schafer K J, Gaarde M B, Heinrich A, Biegert J and Keller U 2004 Strong field quantum path control using attosecond pulse trains *Phys. Rev. Lett.* **92** 023003
[11] Johnsson P, Mauritsson J, Remetter T, L'Huillier A and Schafer K J 2007 Attosecond control of ionization by wave-packet interference *Phys. Rev. Lett.* **99** 233001
[12] Mauritsson J, Johnsson P, Mansten E, Swoboda M, Ruchon T, L'Huillier A and Schafer K J 2008 Coherent electron scattering captured by an attosecond quantum stroboscope *Phys. Rev. Lett.* **100** 073003
[13] Biegert J, Heinrich A, Hauri C P, Kornelis W, Schlup P, Anscombe M, Schafer K J, Gaarde M B and Keller U 2005 Enhancement of high-order harmonic emission using attosecond pulse trains *Laser Phys.* **15** 899–902
[14] Farkas Gy and Tóth Cs 1992 Proposal for attosecond light pulse generation using laser induced multiple-harmonic conversion processes in rare gases *Phys. Lett.* A **168** 447–50
[15] Rundquist A, Durfee III C G, Chang Z, Herne C, Backus S, Murnane M M and Kapteyn H C 1998 Phase-matched generation of coherent soft x-rays *Science* **280** 1412–5
[16] Mairesse Y *et al* 2003 Attosecond synchronization of high-harmonic soft x-rays *Science* **302** 1540–3
[17] Salières P *et al* Feynman's path-integral approach for intense-laser–atom interaction *Science* **292** 902–5
[18] Gaarde M B, Tate J L and Schafer K J 2008 Macroscopic aspects of attosecond pulse generation *J. Phys. B: At. Mol. Opt. Phys.* **41** 132001.1–26
[19] Hostetter J A, Tate J L, Schafer K J and Gaarde M B 2010 Semiclassical approaches to below-threshold harmonics *Phys. Rev.* A **82** 023401
[20] Nicole C, Sluimer I, Rosca-Pruna F, Warntjes M, Vrakking M J J, Bordas Ch, Texier F and Robicheaux F 2000 Slow photoelectron imaging *Phys. Rev. Lett.* **85** 4024–7
[21] Shafir D, Mairesse Y, Villeneuve D M, Corkum P B and Dudovich N 2009 Atomic wavefunctions probed through strong-field light–matter interaction *Nat. Phys.* **5** 412–6